Neuroscience 331 (2016) 197–205

LOSS OF INHIBITION BY BRAIN NATRIURETIC PEPTIDE OVER P2X3 RECEPTORS CONTRIBUTES TO ENHANCED SPIKE FIRING OF TRIGEMINAL GANGLION NEURONS IN A MOUSE MODEL OF FAMILIAL HEMIPLEGIC MIGRAINE TYPE-1

ANNA MARCHENKOVA, [a]
ARN M. J. M. VAN DEN MAAGDENBERG [b,c] **AND ANDREA NISTRI** [a]*

[a] *Neuroscience Department, International School for Advanced Studies (SISSA), Via Bonomea 265, 34136 Trieste, Italy*

[b] *Department of Neurology, Leiden University Medical Centre, Leiden, Netherlands*

[c] *Department of Human Genetics, University Medical Centre, Leiden, Netherlands*

Abstract—Purinergic P2X3 receptors (P2X3Rs) play an important role in pain pathologies, including migraine. In trigeminal neurons, P2X3Rs are constitutively downregulated by endogenous brain natriuretic peptide (BNP). In a mouse knock-in (KI) model of familial hemiplegic migraine type-1 with upregulated calcium $Ca_V2.1$ channel function, trigeminal neurons exhibit hyperexcitability with gain-of-function of P2X3Rs and their deficient BNP-mediated inhibition. We studied whether the absent BNP-induced control over P2X3Rs activity in KI cultures may be functionally expressed in altered firing activity of KI trigeminal neurons. Patch-clamp experiments investigated the excitability of wild-type and KI trigeminal neurons induced by either current or agonists for P2X3Rs or transient receptor potential vanilloid-1 (TRPV1) receptors. Consistent with the constitutive inhibition of P2X3Rs by BNP, sustained pharmacological block of BNP receptors selectively enhanced P2X3R-mediated excitability of wild-type neurons without affecting firing evoked by the other protocols. This effect included increased number of action potentials, lower spike threshold and shift of the firing pattern distribution toward higher spiking activity. Thus, inactivation of BNP signaling transformed the wild-type excitability phenotype into the one typical for KI. BNP receptor block did not influence excitability of KI neurons in accordance with the lack of BNP-induced P2X3R modulation. Our study suggests that, in wild-type trigeminal neurons, negative control over P2X3Rs by the BNP pathway is translated into tonic suppression of P2X3Rs-mediated excitability. Lack of this inhibition in KI cultures results in a hyperexcitability phenotype and might contribute to facilitated trigeminal pain transduction relevant for migraine.

Key words: purinergic receptor, nociception, sensory neurons, TRPV1, vanilloid receptor.

INTRODUCTION

The trigeminal ganglion (TG) is a part of the trigeminovascular system that plays an integral role in regulating pain transduction in primary headache conditions, such as migraine (Noseda and Burstein, 2013). Trigeminal sensory neurons express ATP-gated P2X3 receptors (P2X3Rs) and capsaicin-sensitive transient receptor potential vanilloid-1 (TRPV1) receptors (Vulchanova et al., 1997; Julius and Basbaum, 2001; North, 2003), which mediate nociceptive responses and are thought to contribute to migraine pathophysiology (Yan and Dussor, 2014). Using a knock-in (KI) mouse model, expressing voltage-gated $Ca_V2.1$ channels with the R192Q missense mutation in its α_{1A} subunit that was shown to lead to familial hemiplegic migraine type-1 (FHM1; Ophoff et al., 1996; Ferrari et al., 2015), we have observed a selective upregulation of P2X3Rs function in TG neurons (Nair et al., 2010). This phenomenon is manifested as increased neuronal excitability in response to P2X3Rs activation (Hullugundi et al., 2014). Such results may help to explain the migraine-like pain behavior exhibited by R192Q KI mice (Chanda et al., 2013).

While numerous endogenous modulators upregulate P2X3Rs, to date only brain natriuretic peptide (BNP) and its natriuretic peptide receptor type-A (NPR-A) have been reported to induce constitutive downregulation of P2X3-mediated responses in wild-type (WT) TG neurons (Vilotti et al., 2013; Marchenkova et al., 2015). Indeed, inactivation of BNP signaling with selective NPR-A antagonist anantin or siBNP enhances P2X3Rs-mediated ion currents under voltage clamp conditions, thereby unmasking a background inhibition of P2X3R activity (Vilotti et al., 2013; Marchenkova et al., 2015). Most interestingly, in R192Q KI mice, the BNP-dependent P2X3R modulation appears to be disabled and might contribute to the gain-of-function of R192Q KI trigeminal neurons (Marchenkova et al., 2016). Because

*Corresponding author.
E-mail addresses: marchenkova.anna@sissa.it (A. Marchenkova), maagdenberg@lumc.nl (A. M. J. M. van den Maagdenberg), nistri@sissa.it (A. Nistri).

Abbreviations: α,β-meATP, α,β-methylene adenosine 5-triphosphate; AP, action potential; BDNF, brain-derived neurotrophic factor; BNP, brain natriuretic peptide; CGRP, calcitonin gene-related peptide; FA, fast-adaptive; FHM1, familial hemiplegic migraine type-1; KI, knock-in; MF, multiple-firing; NS, non-spiking; P2X3R, P2X3 receptor; SS, single-spike; TG, trigeminal ganglion; TRPV1, transient receptor potential vanilloid-1; WT, wild type.

http://dx.doi.org/10.1016/j.neuroscience.2016.06.034
0306-4522/

these functional data were obtained by recording membrane currents from neurons, they did not shed light on the neurophysiological correlates of these phenomena as trigeminal sensory neurons encode their responses as a series of action potentials (APs) (Sunada et al., 1990; Chudler et al., 1991; Coste et al., 2008).

The aim of the present study was to find out if BNP/NPR-A-mediated constitutive inhibition of P2X3Rs might actually influence the firing properties of WT neurons. In addition, we wished to explore if BNP acts selectively on P2X3R-mediated activation or on other forms of neuronal depolarization (i.e. current injection- or capsaicin-mediated depolarization). In particular, since the AP threshold is more negative in KI neurons, we investigated whether downregulation of BNP-mediated inhibition might change not only AP patterns but also the readiness to generate APs by shifting the spike threshold to more negative values. All these objectives required a current clamp study.

Thus, in order to uncover any constitutive effect of endogenous BNP, we blocked NPR-A receptors with its selective antagonist anantin (Weber et al., 1991; Yu et al., 2006; Abdelalim and Tooyama, 2011; Vilotti et al., 2013) in analogy with the previously reported protocol (Vilotti et al., 2013). Firing of trigeminal sensory neurons from WT or R192Q KI mice was investigated in response to current pulses as well as brief application of P2X3 or TRPV1 receptor agonists α,β-methylene adenosine 5-triphosphate (α,β-meATP) and capsaicin, respectively (Hullugundi et al., 2014).

Our data suggest that the negative inhibition of P2X3R activity by the BNP/NPR-A pathway results in a decreased P2X3R-mediated excitability of trigeminal neurons in WT cultures. In KI cultures, however, lack of efficient P2X3Rs downregulation contributes to the neuronal hyperexcitability phenotype.

EXPERIMENTAL PROCEDURES

Mouse trigeminal ganglion cultures

Experiments were performed on cultured TG neurons from FHM1 R192Q KI and WT mouse littermates. The colony of KI mice was bred and maintained locally, in accordance with the Italian Animal Welfare Act, after an initial transfer from Leiden University Medical Centre (van den Maagdenberg et al., 2004). All experimental protocols were approved by the SISSA ethics committee and are in accordance with EU guidelines (2010/63/EU) and Italian legislation (D.L. 4/3/2014, No. 26). Every effort was made to minimize the number of animals used for the experiments and their suffering. The genotyping was performed by PCR, as previously reported (Nair et al., 2010) after the mice were sacrificed for culture preparation: hence, at the time of electrophysiological recording the genotype of the tested neurons from each dish was not determined, thus ensuring blind analysis conditions. Primary cultures of P12-P14 mouse TG were prepared as described previously (Simonetti et al., 2006; Hullugundi et al., 2014) and used 24 h after plating. In brief, trigeminal ganglia were isolated from mice killed by cervical dislocation under general anesthesia induced by slowly raising the level of CO_2. Ganglia were cut and dissociated for 12 min at 37 °C in an enzyme mixture containing 0.25 mg/mL trypsin, 1 mg/mL collagenase, and 0.2 mg/mL DNase (Sigma, Milan, Italy) in F-12 medium (Invitrogen Corp, San Giuliano Milanese, Italy). Cells were plated on poly-L-lysine-coated petri dishes in F12 medium with 10% fetal calf serum.

Electrophysiology

After 24 h in culture, trigeminal neurons were superfused continuously (2–3 mL/min) with physiological solution containing (in mM): 152 NaCl, 5 KCl, 1 $MgCl_2$, 2 $CaCl_2$, 10 glucose, and 10 HEPES (pH adjusted to 7.4 with NaOH), as previously described (Nair et al., 2010; Hullugundi et al., 2013). Cells were patch-clamped in the whole-cell configuration, using glass pipettes (4–5 MΩ resistance) filled with the following solution (in mM): 125 K-gluconate, 5 KCl, 2 $MgCl_2$, 2 Mg_2ATP_3, 10 HEPES, and 10 EGTA (pH adjusted to 7.2 with KOH). The K^+ equilibrium potential, calculated with the Nernst equation, was equal to −105 mV, and the liquid junction potential was 14.6 mV. Collected data were corrected accordingly.

Recordings were obtained from small- and medium-sized TG neurons (capacitance below 25 pF) under current-clamp conditions, using a Patch Clamp PC-501A amplifier (Warner Instrument Corporation). Experimental conditions were very similar to those of our previous study (Hullugundi et al., 2014), except for the membrane holding potential, as cells were held at −70 mV (after correction for the liquid junction potential). Electrophysiological responses were filtered at 5 kHz and acquired by means of a DigiData 1200 interface and pClamp 8.2 software (Molecular Devices). Input resistance was measured by applying hyperpolarizing pulses of −5 or −2 pA, while cell capacitance was estimated from the whole-cell capacitance facility.

Depolarizing current pulses lasting for 300 ms with 45 pA amplitude were used to stimulate neurons. As previously shown (Hullugundi et al., 2014), such stimulation is sufficient to elicit cell-specific firing activity from TG neurons of small and medium size. In accordance with our former studies, the P2X3R selective agonist α,β-meATP (Sigma, Milan, Italy) was applied for 2 s using a fast superfusion system (Rapid Solution Changer RSC-200; BioLogic Science Instruments, Claix, France) at a concentration of 10 μM to produce near-maximal P2X3R activation (Sokolova et al., 2006). Capsaicin (Sigma) was applied for 3 s at a concentration of 1 μM to elicit stable TRPV1 receptor-mediated responses (Simonetti et al., 2006; Nair et al., 2010; Hullugundi et al., 2014). The selective NPR-A antagonist anantin (500 nM) was applied to the cultures overnight (24 h) to block NPR-A receptor activity (Yu et al., 2006; Vilotti et al., 2013; Marchenkova et al., 2015); control dishes were incubated for the same period of time without anantin.

Data analysis

Data are expressed as mean ± standard error of the mean, with n indicating the number of analyzed cells.

Data were collected from at least 4 mice for each genotype, and statistical relevance of the sample size (number of analyzed neurons) in each experimental condition was verified with online sample size analysis software biomath.info and powerandsamplesize.com, using power = 0.8 and α (type I error rate) = 0.05. Statistical analysis was performed using Student's *t*-test or the Mann–Whitney rank sum test after the software-directed choice of parametric or nonparametric data, respectively (Matlab; Sigma Plot & Sigma Stat, Chicago, IL, USA) and a chi-square test when analyzing proportion. A *p*-value less than 0.05 was accepted as indicative of a statistically significant difference.

For firing threshold analysis, an algorithm was used that allowed automated threshold detection based on first and second discrete time derivatives of the voltage time-series (Matlab) (Platkiewicz and Brette, 2010; Hullugundi et al., 2014). The parameters used for calculating the exact threshold value were empirically determined and kept constant for all analyzed recordings. The present data were consistent with the formerly reported values (Sekerli et al., 2004; Hullugundi et al., 2014).

RESULTS

Anantin affects firing patterns of WT but not KI trigeminal sensory neurons

In line with previously reported data, we observed four distinct firing patterns in cultured TG neurons after stimulation with 45 pA current pulses (Catacuzzeno et al., 2008; Hullugundi et al., 2014). Fig. 1A shows representative traces obtained from TG neurons with different firing patterns. Single-spike (SS) neurons fired only once at the beginning of the stimulus. Fast-adaptive (FA) cells stopped firing after generating several spikes. Multiple-firing cells (MF) fired during the whole period of stimulation with a time-dependent decrease in spike frequency (adaptation). Rapid-firing neurons (RF) showed sustained high-frequency firing and a large after-hyperpolarization. Finally, a small fraction of neurons did not show any firing activity (non-spiking, NS, cells) in response to 45 pA stimulation (they were, however, responsive to higher intensity stimulation; data not shown). The percent distribution of these firing patterns is shown in Fig. 1B for WT (upper panels) and KI (lower panels) cultures in control (left) and after 24 h application of NPR-A antagonist anantin (500 nM; right). WT and KI spike pattern distributions were similar in control condition, and anantin application did not cause any significant ($p > 0.05$, chi-square test) changes (Fig. 1B).

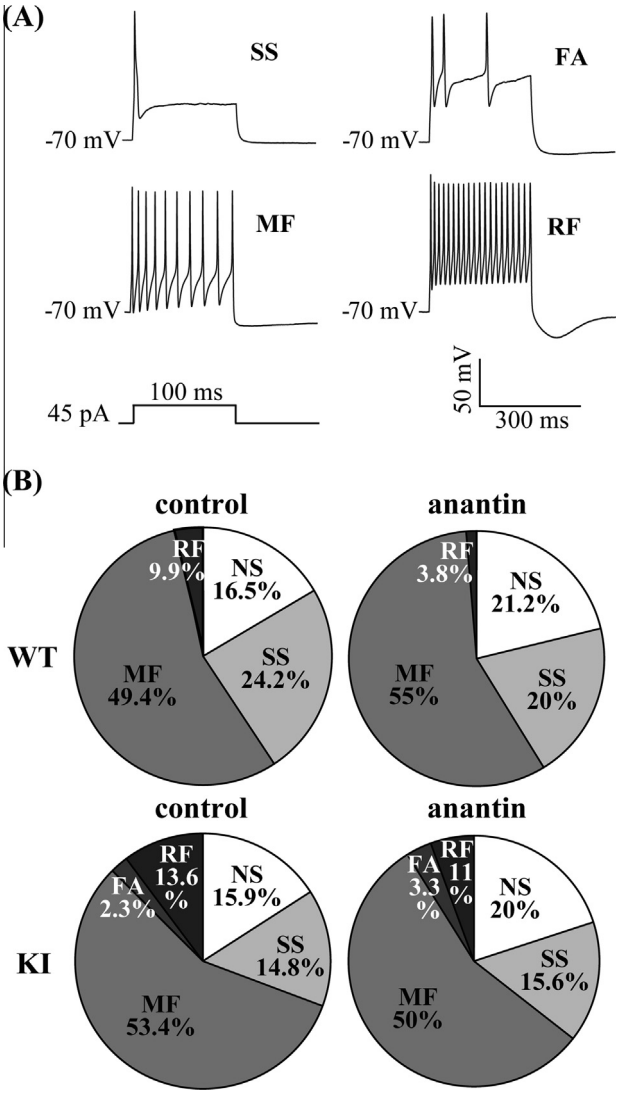

Fig. 1. Firing patterns of trigeminal sensory neurons evoked by intracellular current pulse injections. (A) Representative traces of firing pattern types recorded from wild-type (WT) TG neurons in response to intracellular current pulse injections (45 pA, 300 ms); similar patterns of firing activity were obtained from knock-in (KI) cells. (B) Pie charts show percent distributions of firing patterns in WT and KI TG cultures without (control) and after anantin application (500 nM, 24 h). Cell counts for non-spiking (NS), single-spike (SS), multiple-firing (MF), fast-adaptive (FA), rapid-firing (RF) groups, respectively, are: n (WT, control) = 15, 22, 51, 0, 3; n (WT, after anantin application) = 17, 16, 46, 0, 1; n (KI, control) = 14, 13, 50, 2, 9; n (KI, after anantin application) = 18, 14, 50, 3, 5. Anantin did not change WT or KI firing pattern distributions ($p > 0.05$ for each group, chi-square test).

Under physiological conditions, sensory neurons are readily depolarized by activation of their ionotropic membrane receptors. Thus, TG neurons generate distinct firing patterns mediated by ATP-gated P2X3Rs or TRPV1 receptors (Hullugundi et al., 2014). We next investigated how inactivation of the BNP/BPR-A pathway might affect neuronal firing elicited by the P2X3R agonist α,β-meATP (Jarvis and Khakh, 2009; Fabbretti and Nistri, 2012) or the TRPV1 agonist capsaicin (Meents et al., 2010; O'Neill et al., 2012). Fig. 2A shows representative traces of neuronal responses observed after 2 s pulses of 10 μM α,β-meATP. In view of the fast inactivation of P2X3R currents (North, 2002; Coddou et al., 2011; Giniatullin and Nistri, 2013) that restricts P2X3R-induced firing activity to short spike discharges, application of α, β-meATP evoked SS and MF patterns or just subthreshold depolarization (Fig. 2A). Unlike responses to current stimulation, in case of P2X3R-mediated firing clear differences in firing pattern distribution were observed between WT and KI cultures (Fig. 2B). In comparison with WT, KI

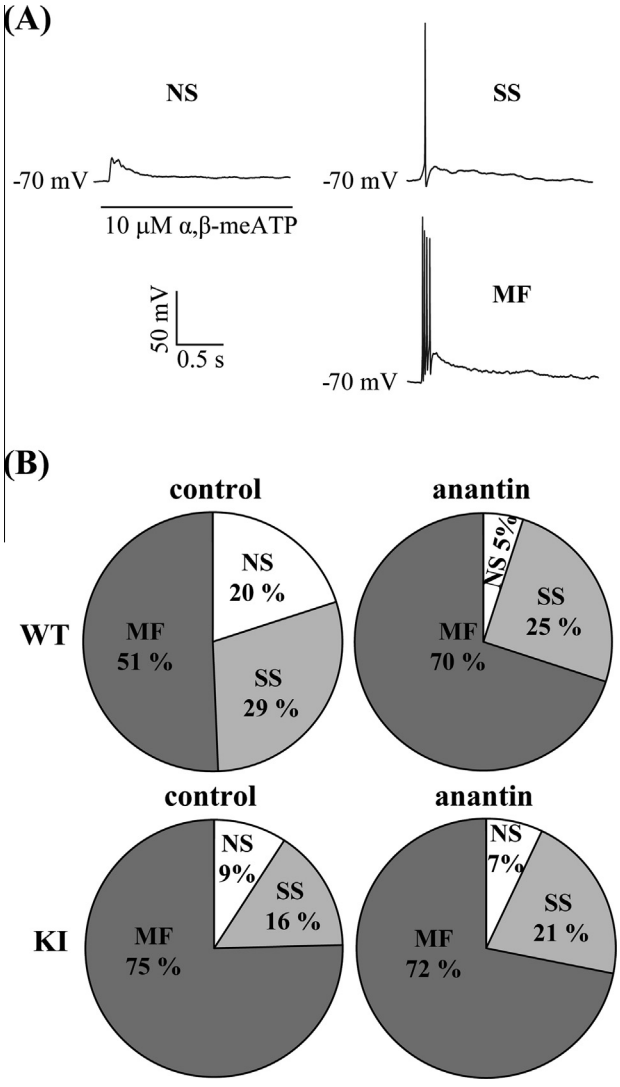

Fig. 2. Firing patterns of trigeminal sensory neurons evoked by α,β-meATP application. (A) Representative traces of firing pattern types recorded from WT TG neurons in response to α,β-meATP pulses (10 μM, 2 s); KI neurons showed similar patterns. (B) Pie charts describe percent distributions of firing patterns in WT and KI TG cultures without (control) and after anantin application (500 nM, 24 h). Note significantly lower number of multiple-firing (MF) neurons under control conditions in WT (upper left) versus KI (bottom left) cultures ($p = 0.003$, chi-square test). After anantin application (right diagrams) the WT firing pattern distribution becomes statistically indistinguishable from that of KI ($p > 0.05$ for each group, chi-square test), with increased number of WT MF cells compared to control ($p = 0.014$, chi-square test). Cell counts for non-spiking (NS), single-spike (SS) and MF groups, respectively, are: n (WT, control) = 15, 22, 38; n (WT, after anantin application) = 4, 20, 56; n (KI, control) = 6, 10, 49; n (KI, after anantin application) = 5, 15, 51.

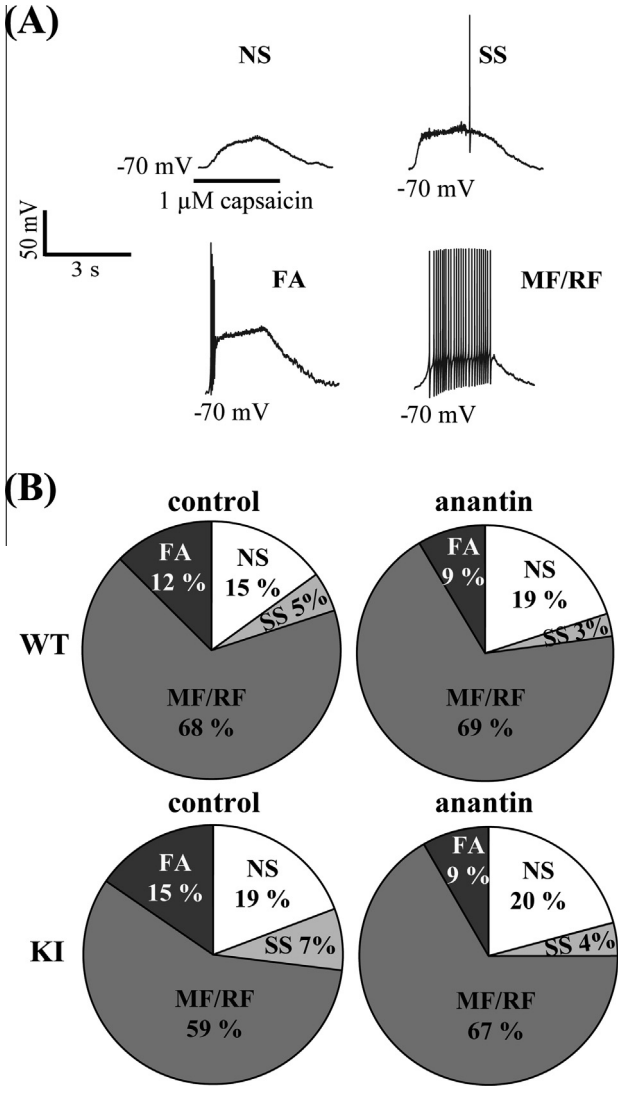

Fig. 3. Firing patterns of trigeminal sensory neurons evoked by capsaicin. (A) Representative traces of firing pattern types recorded from WT TG neurons in response to capsaicin pulses (1 μM, 3 s); similar patterns of firing activity were recorded from KI cells. (B) Pie charts show percent distributions of firing patterns in WT and KI TG cultures without (control) and after anantin application (500 nM, 24 h). Cell counts for non-spiking (NS), single-spike (SS), fast-adaptive (FA), multiple-firing/rapid-firing (MF/RF) groups, respectively, are: n (WT, control) = 6, 2, 5, 27; n (WT, after anantin application) = 7, 1, 3, 24; n (KI, control) = 5, 2, 4, 15; n (KI, after anantin application) = 5, 1, 2, 16. Anantin did not change WT or KI firing pattern distributions ($p > 0.05$ for each group, chi-square test).

cultures showed a much larger number of MF neurons (75 % in KI *vs* 51 % in WT; $p = 0.003$, chi-square test) and, correspondingly, decreased numbers of NS + SS neurons (Fig. 2B, left diagrams; $p = 0.003$, chi-square test). It is noteworthy that anantin treatment (500 nM; 24 h) changed the WT distribution profile to that observed in KI cultures, namely, it strongly increased population size of MF neurons ($p = 0.014$, chi-square test), and decreased number of low firing cells (Fig. 2B, upper diagrams; $p = 0.004$ for NS group, $p = 0.014$ for NS + SS group; chi-square test). Notably, anantin application failed to induce significant changes in the KI distribution (compare bottom diagrams in Fig. 2B).

We next investigated firing activity of TG neurons induced by short pulses of capsaicin (1 μM, 3 s) as summarized in Fig. 3. When stimulated by capsaicin, both WT and KI neurons produced similar types of responses (Fig. 3A) with similar distributions (Fig. 3B, diagrams on the left) which were not altered by anantin application (Fig. 3B, diagrams on the right). This shows that the BNP pathway in TG neurons did not regulate firing evoked by TRPV1 receptor activation.

Anantin selectively increases spike number during P2X3-mediated firing in WT TG cells

The number of spikes generated by a given chemical stimulus is one of the main parameters to convey activation of brainstem trigeminal nuclei as it determines transmitter release properties of afferent cells (Coste et al., 2008). Thus, we investigated whether 24 h anantin application not only changes the firing pattern distribution but also the number of spikes that WT and KI neurons can generate, as this property can be regarded as an indication of more efficient nociceptive signaling. Representative α,β-meATP-dependent firing responses are shown in Fig. 4A. In control Krebs solution, the mean number of spikes across all WT cells was statistically lower than in KI cells (Fig. 4B; compare open with filled circles). In particular, this effect was observed for MF group (Fig. 4C). Thus, the difference between WT and KI neurons regarding the average number of generated APs in response to α,β-meATP application originated both from a higher percent of MF cells in KI culture and an increased spike count in the KI MF population.

Notably, anantin application increased average spike count of WT cells to that of KI cells (Fig. 4B, D $p < 0.05$, Mann–Whitney rank sum test). In particular, the number of spikes of WT MF cells grew in response to anantin application (Fig. 4C) that was accompanied

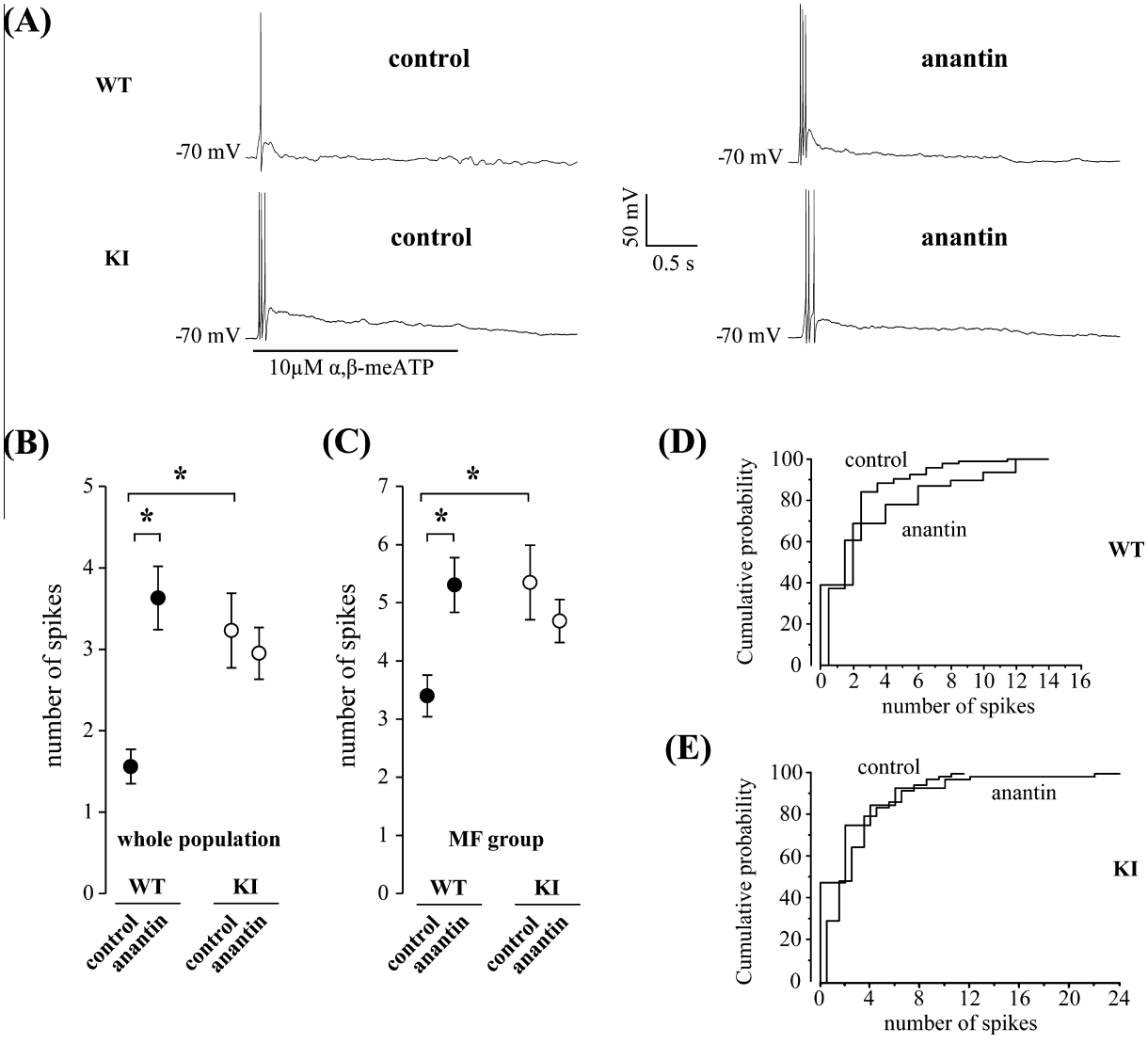

Fig. 4. Anantin increases number of spikes generated by WT neurons in response to α,β-meATP application. (A) Representative traces recorded from WT and KI TG neurons in response to α,β-meATP pulses (10 μM, 2 s) without (control) and after anantin application (24 h, 500 nM). Note the similarity of the WT and KI firing profiles after anantin treatment. (B) Quantification of the average spike counts for the whole WT (closed circles) and KI (opened circles) populations without (control) and after anantin application; n (WT, control) = 75; n (WT, anantin) = 80; n (KI, control) = 65; n (KI, anantin) = 71; $p < 0.05$, Mann–Whitney rank sum test. (C) The diagram quantifies the mean number of spikes for the WT and KI MF neurons; n = (WT, control) = 38; n (WT, anantin) = 56; n (KI, control) = 49; n (KI, anantin) = 51; $p < 0.05$, Mann–Whitney rank sum test. Note the similar number of spikes in KI (both without (control) and after anantin) and WT after anantin application. (D) Kolmogorov–Smirnov plots of cumulative firing probability for WT neurons without (control) and after anantin application. (E) Kolmogorov–Smirnov plots of the cumulative firing probability for KI neurons without (control) and after anantin application.

by a rightward shift in the cumulative probability plot for the WT firing responses after anantin (Fig. 4D). This observation is consistent with the previously reported enhancement in P2X3R membrane currents after anantin application to WT (Vilotti et al., 2013; Marchenkova et al., 2015). In KI cultures, in analogy to the unchanged firing pattern distribution (Fig. 2B), anantin did not alter the mean value and the cumulative probability plot for the spike count (Fig. 4B, C, open circles; Fig. 4E).

Unlike what was seen with α,β-meATP application, whether excitation was induced by a depolarizing current pulse (Fig. 5A) or capsaicin (Fig. 5B), KI and WT cells produced on average similar number of spikes in control as well as after anantin application. These results highlighted the selectivity of BNP pathway modulation on P2X3R-mediated firing.

Anantin selectively decreases spike threshold for P2X3-dependent firing in WT TG cells

It has previously been shown that the hyperexcitability phenotype in R192Q KI TG is associated with a lower threshold for α,β-meATP-evoked firing (Hullugundi et al., 2014). We, therefore, set out to study threshold values of WT and KI neurons in order to find out whether there was a differential response to 24 h 500 nM anantin treatment. Threshold values for α,β-meATP-, depolarizing current- or capsaicin-induced firing in each experimental condition are illustrated in Fig. 6A–C, respectively. Control threshold values in KI were lower than in WT for α,β-meATP- and current-evoked spikes (Fig. 6A, B; $p < 0.05$, Mann–Whitney rank sum test). Anantin treatment (500 nM, 24 h) produced a statistically significant shift of the mean WT threshold value toward more negative voltage typical for KI neurons, but only in case of α,β-meATP-mediated firing (Fig. 6A, closed circles; $p < 0.05$, Mann–Whitney rank sum test). Indeed, spike threshold of treated WT cells became statistically indistinguishable from that of KI cells (Fig. 6A). In particular, Fig. 6D exemplifies different threshold levels (see arrows) for WT and KI neurons stimulated with α,β-meATP. It is noteworthy that anantin had no effect on KI cells (Fig. 6A, D). In the case of capsaicin-evoked APs, no statistically significant differences in spike threshold values were detected between control and anantin-treated WT and KI trigeminal neurons (Fig. 6C).

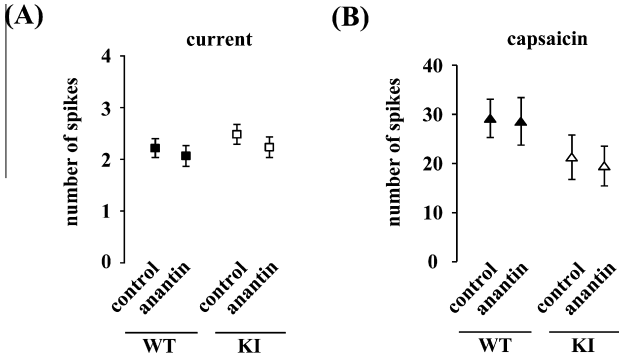

Fig. 5. Anantin does not change number of spikes generated in response to capsaicin or current pulse injections. The graphs compare average spike counts of WT or KI neurons without (control) and after anantin application for (A) current pulse stimulation (45 pA, 300 ms) or (B) capsaicin (1 μM, 3 s). Cell counts for current stimulation: n (WT, control) = 91; n (WT, anantin) = 80; n (KI, control) = 88; n (KI, anantin) = 90. Cell counts for capsaicin stimulation: n (WT, control) = 40; n (WT, anantin) = 35; n (KI, control) = 26; n (KI, anantin) = 24.

DISCUSSION

The principal finding of this study is the observation that sustained inactivation of the BNP/NPR-A pathway in WT TG cultures selectively elevated P2X3R-dependent neuronal firing up to the level observed in TG cultures of the FHM1 R192Q KI mouse model. In WT neurons, under basal conditions, the NPR-A pathway appears to be activated by endogenous BNP (Marchenkova et al., 2015), which constitutively inhibits neuronal excitability mediated by P2X3Rs. Furthermore, we showed that the hyperexcitability phenotype that is typical for trigeminal sensory neurons of KI mice (Hullugundi et al., 2014) originated from the apparent lack of BNP/NPR-A-mediated regulation and primarily concerned P2X3R-mediated firing.

Differences between WT and KI trigeminal sensory neurons

Considering firing patterns in response to intracellular current pulse injection, four types were distinguished in both WT and KI trigeminal small- to medium-size neurons. Consistent with our previous study (Hullugundi et al., 2014), in case of capsaicin stimulation no significant differences were detected between WT and KI cultures in terms of the firing pattern distribution, the average number of spikes, or the threshold for generating APs. Block of BNP/NPR-A signaling caused no change in these excitability parameters when neurons were stimulated by either capsaicin or current injection, implicating that the BNP/NPR-A pathway of TG neurons did not affect voltage-gated ion channels or TRPV1-dependent excitability.

Major differences were, however, observed between P2X3R-mediated firing of WT and KI cultures. The hyperexcitability profile of KI neurons (Hullugundi et al., 2014) was expressed as a combination of interrelated parameters, i.e. a higher percent of MF neurons, an increased average number of APs, and a decreased voltage threshold for α,β-meATP-induced firing. These phenomena can be explained by the fact that P2X3R function is upregulated in KI TG, whereas TRPV1 responses remain at the same level (Nair et al., 2010). There are many well-known endogenous modulators, such as calcitonin gene-related peptide (CGRP), nerve growth factor (NGF), brain-derived neurotrophic factor (BDNF), and tumor necrosis factor alpha (TNFα), that upregulate P2X3R function in normal and pathological conditions (Fabbretti and Nistri, 2012), and, therefore, may influence neuronal excitability. In particular, elevated levels of CGRP and BDNF are suggested to contribute to the observed P2X3R gain-of-function in KI trigeminal neurons (Ceruti et al., 2011; Hullugundi et al., 2013). More

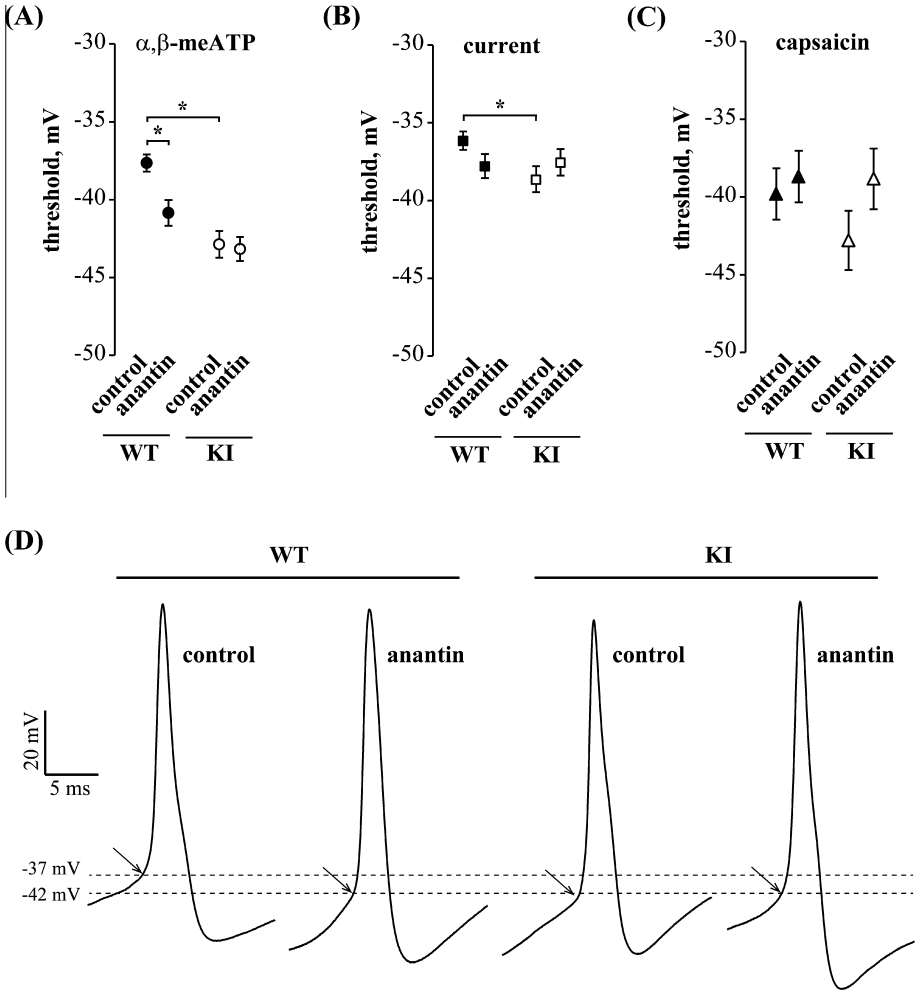

Fig. 6. Anantin decreases threshold for spikes evoked by α,β-meATP in WT neurons. (A) Diagram shows average threshold values for WT and KI neurons without (control) and after anantin application (500 nm, 24 h) for APs evoked by α,β-meATP (10 μM, 2 s). Note that WT threshold after anantin application comes close to the KI values. $^{*}p < 0.05$, Mann–Whitney rank sum test. Numbers of analyzed neurons are: n (WT, control) = 60; n (WT, anantin) = 76; n (KI, control) = 59; n (KI, anantin) = 66. (B) Average threshold values for WT and KI neurons without (control) and after anantin application (500 nm, 24 h) for APs evoked by 300 ms 45 pA current pulse. Anantin does not significantly change WT or KI threshold values. Numbers of analyzed neurons are: n (WT, control) = 76; n (WT, anantin) = 63; n (KI, control) = 74; n (KI, anantin) = 72. (C) Diagram shows no difference in average threshold values for WT and KI neurons between untreated (control) and anantin-treated (500 nm, 24 h) neurons for APs evoked by capsaicin (1 μM, 3 s). Numbers of analyzed neurons are: n (WT, control) = 34; n (WT, anantin) = 28; n (KI, control) = 21; n (KI, anantin) = 19. (D) Representative traces of first AP generated in response to α,β-meATP (10 μM, 2 s); arrows indicate firing threshold. Note that the WT threshold after anantin application becomes more negative and comes close to the threshold observed in KI.

recently, BNP was reported to be the first negative regulator of P2X3Rs in TG cells (Vilotti et al., 2013; Marchenkova et al., 2015). BNP, through its receptor NPR-A, constitutively suppresses P2X3R currents in WT trigeminal neurons via a dual process comprising an increased P2X3R serine phosphorylation and a redistribution of the receptors to non-lipid raft membrane compartments (Marchenkova et al., 2015). Ambient concentrations of BNP are sufficient to maximize the P2X3R inhibition that can be readily unveiled by applying the NPR-A antagonist anantin (Vilotti et al., 2013; Marchenkova et al., 2015). A subsequent study has demonstrated that, in KI neurons of the FHM1 mouse model, the BNP/NPR-A control over P2X3R activity is inefficient despite normal expression of NPR-A receptors and the presence of BNP-releasing cells (Marchenkova et al., 2016). The main question, therefore, was whether the BNP-dependent inhibitory effect over P2X3Rs in WT is translated into selective downregulation of P2X3R-mediated firing and whether lack of such inhibition in KI contributes to the KI hyperexcitability phenotype.

Anantin converts WT low excitability to KI hyperexcitability

Recent studies have proposed BNP as a potential endogenous anti-inflammatory and anti-pain modulator, which, acting through its receptor NPR-A, inhibits the excitability of sensory DRG neurons and constantly downregulates P2X3Rs in TG cells (Zhang et al., 2010; Marchenkova et al., 2015). In the present study, we obtained supportive evidence that the BNP/NPR-A pathway plays an important selective role in restraining P2X3R-dependent excitability of TG neurons. Being a

synthetic analog of the natural P2X3R ligand ATP, α,β-meATP simulates a situation in which ATP is released in a pulsatile manner, often together with other neurotransmitters or after mechanical stress (Fabbretti, 2013). Enhanced ATP synthesis/release in pathological conditions, including migraine (Burnstock et al., 2011), is thought to support the process of neuronal sensitization (Hamilton and McMahon, 2000). Thus, a system that restrains ATP-gated receptors and, in particular, P2X3Rs expressed by nociceptive neurons, could serve as an intrinsic mechanism to avoid sensitization and prevent overactivation of sensory neurons. Future *in vivo* experiments are necessary to support this idea.

Inhibition of NPR-A receptors with their selective antagonist anantin led to significant changes in WT α,β-meATP-mediated excitability. Anantin application decreased the spike threshold, increased the average number of generated APs in TG neurons and changed the distribution of firing patterns in WT cultures toward higher excitability patterns. Altogether, BNP/NPR-A pathway inactivation transformed WT excitability profile to the one typically associated with KI TG phenotype. Hence, under normal conditions in WT TG, endogenous BNP acting via NPR-A (Marchenkova et al., 2015) constitutively restrains the activity of P2X3Rs and, as a consequence, P2X3R-mediated neuronal excitability as well. In the R192Q KI mouse model, the BNP/NPR-A pathway, albeit normally expressed, is unable to overcome the strong upregulation of P2X3Rs by enhanced CGRP levels (Marchenkova et al., 2016), leading to the increased excitability in response to P2X3R activation.

It is interesting to compare the contrasting actions by BNP and CGRP on P2X3Rs. While BNP stimulates cGMP synthesis in TG neurons (Vilotti et al., 2013) and, thus, changes P2X3R membrane distribution and phosphorylation state (Marchenkova et al., 2015), CGRP facilitates release of BDNF (Simonetti et al., 2008) and stimulates cAMP to phosphorylate CREB and promote P2X3R neosynthesis. Thus, the overall effect of CGRP is more persistent (Fabbretti et al., 2006) and is compatible with enhanced excitability of KI TG neurons, especially because of the upregulated constitutive release of this peptide (Ceruti et al., 2011; Hullugundi et al., 2013). Future studies are necessary to establish whether KI TG neurons in culture retain the poor sensitivity to nitrates as observed in patients suffering from FHM-1 (Hansen et al., 2008).

Processes underlying changes in P2X3R-mediated firing

A striking observation was that the effects evoked by anantin were highly selective, targeting only P2X3R-mediated excitability. While higher efficiency of P2X3Rs may be attributed to discrete changes in their molecular properties (Fabbretti and Nistri, 2012), the negative shift in the spike threshold after anantin treatment is more difficult to explain. There are no apparent differences in passive membrane properties after anantin application that might provide a biophysical explanation for this phenomenon (Marchenkova et al., 2015). One hypothesis is that P2X3Rs might become more closely clustered with voltage-gated channels responsible for the subthreshold behavior of sensory neurons. A complementary view is that a large number of nociceptive neurons specifically express a certain type of subthreshold Na^+ channel that increases the probability to reach the threshold for firing APs by facilitating the voltage trajectory to spike discharge (Dib-Hajj et al., 2013). Whether facilitated association between P2X3Rs and certain subtypes of Na^+ channels is sequential to experimental block of BNP receptors deserves future investigation.

CONCLUSIONS

One important conclusion arising from the present report is that BNP/NPR-A-dependent inhibition is restricted to only one class of chemical nociception mediated by ATP-gated channels. Broad spectrum anti-nociception cannot be, therefore, assumed to occur by enhancing the BNP/NPR-A pathway that might be theoretically useful only when P2X3R signaling is selectively enhanced. When P2X3R inhibition is swamped by the constitutive hyperactivity as seen in KI neurons of the FHM1 mouse model, migraine-like pain behavior may emerge with characteristics conferred by overactive P2X3Rs (Fabbretti and Nistri, 2012).

Acknowledgments—This work was supported by the EU FP7 grant EuroHeadPain (#602633; A.M.J.M.vdM. and A.N.). All authors read and approved the final manuscript. A.M. designed the experiments and collected the data; A.M.J.M.vdM. supplied the genetic mouse model; A.N. supervised the project; A.M., A. N., and A.M.J.M.VDM. wrote/revised the manuscript.

REFERENCES

Abdelalim EM, Tooyama I (2011) NPR-A regulates self-renewal and pluripotency of embryonic stem cells. Cell Death Dis 2:e127.

Burnstock G, Krügel U, Abbracchio MP, Illes P (2011) Purinergic signalling: from normal behaviour to pathological brain function. Prog Neurobiol 95:229–274.

Catacuzzeno L, Fioretti B, Pietrobon D, Franciolini F (2008) The differential expression of low-threshold K^+ currents generates distinct firing patterns in different subtypes of adult mouse trigeminal ganglion neurones. J Physiol 586:5101–5118.

Ceruti S, Villa G, Fumagalli M, Colombo L, Magni G, Zanardelli M, Fabbretti E, Verderio C, van den Maagdenberg AMJM, Nistri A, Abbracchio MP (2011) Calcitonin gene-related peptide-mediated enhancement of purinergic neuron/glia communication by the algogenic factor bradykinin in mouse trigeminal ganglia from wild-type and R192Q Cav2.1 knock-in mice: implications for basic mechanisms of migraine pain. J Neurosci 31:3638–3649.

Chanda ML, Tuttle AH, Baran I, Atlin C, Guindi D, Hathaway G, Israelian N, Levenstadt J, Low D, Macrae L, O'Shea L, Silver A, Zendegui E, Mariette Lenselink A, Spijker S, Ferrari MD, van den Maagdenberg AMJM, Mogil JS (2013) Behavioral evidence for photophobia and stress-related ipsilateral head pain in transgenic Cacna1a mutant mice. Pain 154:1254–1262.

Chudler EH, Foote WE, Poletti CE (1991) Responses of cat C1 spinal cord dorsal and ventral horn neurons to noxious and non-noxious stimulation of the head and face. Brain Res 555:181–192.

Coddou C, Yan Z, Obsil T, Huidobro-Toro JP, Stojilkovic SS (2011) Activation and regulation of purinergic P2X receptor channels. Pharmacol Rev 63:641–683.

Coste J, Voisin DL, Luccarini P, Dallel R (2008) A role for wind-up in trigeminal sensory processing: intensity coding of nociceptive stimuli in the rat. Cephalalgia Int J Headache 28:631–639.
Dib-Hajj SD, Yang Y, Black JA, Waxman SG (2013) The Nav1.7 sodium channel: from molecule to man. Nat Rev Neurosci 14:49–62.
Fabbretti E (2013) ATP P2X3 receptors and neuronal sensitization. Front Cell Neurosci 7:236.
Fabbretti E, D'Arco M, Fabbro A, Simonetti M, Nistri A, Giniatullin R (2006) Delayed upregulation of ATP P2X3 receptors of trigeminal sensory neurons by calcitonin gene-related peptide. J Neurosci 26:6163–6171.
Fabbretti E, Nistri A (2012) Regulation of P2X3 receptor structure and function. CNS Neurol Disord Drug Targets 11:687–698.
Ferrari MD, Klever RR, Terwindt GM, Ayata C, van den Maagdenberg AMJM (2015) Migraine pathophysiology: lessons from mouse models and human genetics. Lancet Neurol 14:65–80.
Giniatullin R, Nistri A (2013) Desensitization properties of P2X3 receptors shaping pain signaling. Front Cell Neurosci 7:245.
Hamilton SG, McMahon SB (2000) ATP as a peripheral mediator of pain. J Auton Nerv Syst 81:187–194.
Hansen JM, Thomsen LL, Olesen J, Ashina M (2008) Familial hemiplegic migraine type 1 shows no hypersensitivity to nitric oxide. Cephalalgia Int J Headache 28:496–505.
Hullugundi SK, Ansuini A, Ferrari MD, van den Maagdenberg AMJM, Nistri A (2014) A hyperexcitability phenotype in mouse trigeminal sensory neurons expressing the R192Q Cacna1a missense mutation of familial hemiplegic migraine type-1. Neuroscience 266:244–254.
Hullugundi SK, Ferrari MD, van den Maagdenberg AMJM, Nistri A (2013) The mechanism of functional up-regulation of P2X3 receptors of trigeminal sensory neurons in a genetic mouse model of familial hemiplegic migraine type 1 (FHM-1). PLoS ONE 8:e60677.
Jarvis MF, Khakh BS (2009) ATP-gated P2X cation-channels. Neuropharmacology 56:208–215.
Julius D, Basbaum AI (2001) Molecular mechanisms of nociception. Nature 413:203–210.
Marchenkova A, Vilotti S, Fabbretti E, Nistri A (2015) Brain natriuretic peptide constitutively downregulates P2X3 receptors by controlling their phosphorylation state and membrane localization. Mol Pain 11:71.
Marchenkova A, Vilotti S, Ntamati N, van den Maagdenberg AM, Nistri A (2016) Inefficient constitutive inhibition of P2X3 receptors by brain natriuretic peptide system contributes to sensitization of trigeminal sensory neurons in a genetic mouse model of familial hemiplegic migraine. Mol Pain 12:1–12.
Meents JE, Neeb L, Reuter U (2010) TRPV1 in migraine pathophysiology. Trends Mol Med 16:153–159.
Nair A, Simonetti M, Birsa N, Ferrari MD, van den Maagdenberg AMJM, Giniatullin R, Nistri A, Fabbretti E (2010) Familial hemiplegic migraine Cav2.1 channel mutation R192Q enhances ATP-gated P2X3 receptor activity of mouse sensory ganglion neurons mediating trigeminal pain. Mol Pain 6:48.
North RA (2002) Molecular physiology of P2X receptors. Physiol Rev 82:1013–1067.
North RA (2003) The P2X3 subunit: a molecular target in pain therapeutics. Curr Opin Investig Drugs 4:833–840.
Noseda R, Burstein R (2013) Migraine pathophysiology: anatomy of the trigeminovascular pathway and associated neurological symptoms CSD sensitization and modulation of pain. Pain 154 (Suppl. 1).
O'Neill J, Brock C, Olesen AE, Andresen T, Nilsson M, Dickenson AH (2012) Unravelling the mystery of capsaicin: a tool to understand and treat pain. Pharmacol Rev 64:939–971.
Ophoff RA, Terwindt GM, Vergouwe MN, van Eijk R, Oefner PJ, Hoffman SMG, Lamerdin JE, Mohrenweiser HW, Bulman DE, Ferrari M, Haan J, Lindhout D, van Ommen G-JB, Hofker MH, Ferrari MD, Frants RR (1996) Familial hemiplegic migraine and episodic ataxia type-2 are caused by mutations in the Ca^{2+} channel gene CACNL1A4. Cell 87:543–552.
Platkiewicz J, Brette R (2010) A threshold equation for action potential initiation. PLoS Comput Biol 6:e1000850.
Sekerli M, Del Negro CA, Lee RH, Butera RJ (2004) Estimating action potential thresholds from neuronal time-series: new metrics and evaluation of methodologies. IEEE Trans Biomed Eng 51:1665–1672.
Simonetti M, Fabbro A, D'Arco M, Zweyer M, Nistri A, Giniatullin R, Fabbretti E (2006) Comparison of P2X and TRPV1 receptors in ganglia or primary culture of trigeminal neurons and their modulation by NGF or serotonin. Mol Pain 2:11.
Simonetti M, Giniatullin R, Fabbretti E (2008) Mechanisms mediating the enhanced gene transcription of P2X3 receptor by calcitonin gene-related peptide in trigeminal sensory neurons. J Biol Chem 283:18743–18752.
Sokolova E, Skorinkin A, Moiseev I, Agrachev A, Nistri A, Giniatullin R (2006) Experimental and modeling studies of desensitization of P2X3 receptors. Mol Pharmacol 70:373–382.
Sunada T, Kurasawa I, Hirose Y, Nakamura Y (1990) Intracellular response properties of neurons in the spinal trigeminal nucleus to peripheral and cortical stimulation in the cat. Brain Res 514:189–197.
van den Maagdenberg AMJM, Pietrobon D, Pizzorusso T, Kaja S, Broos LAM, Cesetti T, van de Ven RCG, Tottene A, van der Kaa J, Plomp JJ, Frants RR, Ferrari MD (2004) A cacna1a knockin migraine mouse model with increased susceptibility to cortical spreading depression. Neuron 41:701–710.
Vilotti S, Marchenkova A, Ntamati N, Nistri A (2013) B-type natriuretic peptide-induced delayed modulation of TRPV1 and P2X3 receptors of mouse trigeminal sensory neurons. PLoS ONE 8: e81138.
Vulchanova L, Riedl MS, Shuster SJ, Buell G, Surprenant A, North RA, Elde R (1997) Immunohistochemical study of the P2X2 and P2X3 receptor subunits in rat and monkey sensory neurons and their central terminals. Neuropharmacology 36:1229–1242.
Weber W, Fischli W, Hochuli E, Kupfer E, Weibel EK (1991) Anantin–a peptide antagonist of the atrial natriuretic factor (ANF). I. Producing organism, fermentation, isolation and biological activity. J Antibiot (Tokyo) 44:164–171.
Yan J, Dussor G (2014) Ion channels and migraine. Headache 54:619–639.
Yu Y-C, Cao L-H, Yang X-L (2006) Modulation by brain natriuretic peptide of GABA receptors on rat retinal ON-type bipolar cells. J Neurosci Off J Soc Neurosci 26:696–707.
Zhang F-X, Liu X-J, Gong L-Q, Yao J-R, Li K-C, Li Z-Y, Lin L-B, Lu Y-J, Xiao H-S, Bao L, Zhang X-H, Zhang X (2010) Inhibition of inflammatory pain by activating B-type natriuretic peptide signal pathway in nociceptive sensory neurons. J Neurosci 30:10927–10938.

(Accepted 18 June 2016)
(Available online 23 June 2016)